Taylor & Francis
Taylor & Francis Group

Journal of Biomolecular Structure and Dynamics

ISSN: (Print) (Online) Journal homepage: https://www.tandfonline.com/loi/tbsd20

An efficient synthesis of novel di-heterocyclic benzazole derivatives and evaluation of their antiproliferative activities

Oztekin Algul, Ronak Haj Ersan, Mehmet Abdullah Alagoz, Nizami Duran & Serdar Burmaoglu

To cite this article: Oztekin Algul, Ronak Haj Ersan, Mehmet Abdullah Alagoz, Nizami Duran & Serdar Burmaoglu (2021) An efficient synthesis of novel di-heterocyclic benzazole derivatives and evaluation of their antiproliferative activities, Journal of Biomolecular Structure and Dynamics, 39:18, 6926-6938, DOI: 10.1080/07391102.2020.1803966

To link to this article: https://doi.org/10.1080/07391102.2020.1803966

JOURNAL OF BIOMOLECULAR STRUCTURE AND DYNAMICS
2021, VOL. 39, NO. 18, 6926–6938
https://doi.org/10.1080/07391102.2020.1803966

An efficient synthesis of novel di-heterocyclic benzazole derivatives and evaluation of their antiproliferative activities

Oztekin Algul[a], Ronak Haj Ersan[a], Mehmet Abdullah Alagoz[b], Nizami Duran[c] and Serdar Burmaoglu[d]

[a]Department of Pharmaceutical Chemistry, Faculty of Pharmacy, Mersin University, Mersin, Turkey; [b]Department of Pharmaceutical Chemistry, Faculty of Pharmacy, Inonu University, Malatya, Turkey; [c]Department of Medical Microbiology, Medical Faculty, Mustafa Kemal University, Antakya-Hatay, Turkey; [d]Department of Chemistry, Faculty of Science, Atatürk University, Erzurum, Turkey

Communicated by Ramaswamy H. Sarma

ABSTRACT

A series of unsymmetrical nine di-heterocyclic compounds of benzazole derivatives were synthesized at one step via cyclization reaction. The compounds evaluated for *in vitro* cytotoxic activity against A549, A498, HeLa, and HepG2 cancer cell lines. The biological evaluation results show that **23, 26** and **29** exhibit better activity against HepG2 and HeLa cancer cell lines. Compound **23** also showed good activity against A549, and A498 cancer cell lines. The analogs were further performed molecular docking studies against human cytochrome P450 2C8 monooxygenase enzyme, calculated some theoretical quantum parameters, ADMET descriptor and molecular electrostatic potential analysis. The strategy applied in this research work may act as a perspective for the rational design of potential anticancer drugs.

Abbreviations: dppb: 1,4-bis(diphenylphosphino)butane; DMF: N,N-dimethylformamide; DMSO: dimethyl sulfoxide; HepG2: human hepatocellular cancer cell line; A498: human renal cancer cell line; A549: human lung adenocarcinoma epithelial cancer cell line; HeLa: human cervical cancer cell line; ADME: absorption, distribution, metabolism, and excretion; ADMET: absorption, distribution, metabolism, excretion and toxicity; MEP: molecular electrostatic potential; MM2: molecular mechanics method; DFT: density functional theory; *HOMO*: highest occupied molecular orbital; *LUMO*: lowest unoccupied molecular orbitals; Egap: energy gap; EA: electron affinity energy; QSAR: quantitative structure–activity relationship; *LOO*: leave-one-out; Sreg: standard deviation of regression; F: Fisher's F value; q^2: correlation coefficient; ROS: reactive oxygen species; XP: extra precision; TLC: thin layer chromatography; PPA: polyphosphoric acid; IC_{50}: the 50% inhibitory concentration; eq: equivalent; Vero: African green monkey kidney epithelial; MTX: methotrexate

ARTICLE HISTORY
Received 11 June 2020
Accepted 26 July 2020

KEYWORDS
Di-heterocyclic structure; benzimidazole; benzothiazole; benzoxazole; benzazole; polyphosphoric acid; antiproliferative activity; molecular docking; ADMET

1. Introduction

The incidence and mortality of cancer are rapidly growing worldwide. According to the World Health Organization, the global cancer burden was estimated to have been 18.1 million new cases and 9.6 million deaths in 2018 (Siegel et al., 2019). In cancer drug discovery programs, researchers have used many novel synthetic compounds as anticancer drugs. Benzazole derivatives (e.g. benzimidazole, benzothiazole, and benzoxazole) have a wide range of biological applications (Noel et al., 2013). The antitumor activity of benzazoles is well documented (Liu et al., 2019; Madia et al., 2018) and there have been several reports in which the benzazole nucleus is modified to improve the antitumor activity (Aiello et al., 2008; Dubey et al., 2006; White et al., 2004). In addition, benzazoles have been reported in the literature to increase the antioxidant level of the organism (Can-Eke et al., 1998; Cressier et al., 2009; Han et al., 2018). In the literature, there is a relationship between antioxidants and cancer in clinical studies. Oxidative stress plays an important role in the pathogenesis of cancer. The levels of reactive oxygen species (ROS) and the capacity of oxidative defenses are well balanced in the cells of healthy individuals. Also, many factors can disrupt this balance and increase the risk of developing cancer (Himmetoglu et al., 2009). Therefore, drugs possessing antioxidant and free radical scavenging properties are considered for preventing and/or treatment of tumor diseases which are directly related to the lack of the antioxidant capacity of the organism.

Bis- and di-heterocyclic benzazole compounds exhibit more potent activities, such as antitumor (Mabkhot et al., 2013; Thurston et al., 1996) and antimicrobial activities (Shaker, 1999) than monomeric compounds owing to their two heterocyclic nuclei. For instance, UK-1 (**1**) and AJI95618 (**2**) are di-heterocyclic benzoxazole derivatives and Ueki *et al.* and Sato *et al.* have demonstrated the cytotoxic activity of

CONTACT Oztekin Algul oztekinalgul@mersin.edu.tr Department of Pharmaceutical Chemistry, Faculty of Pharmacy, Mersin University, Mersin, 33169, Turkey

Supplemental data for this article can be accessed online at https://doi.org/10.1080/07391102.2020.1803966.

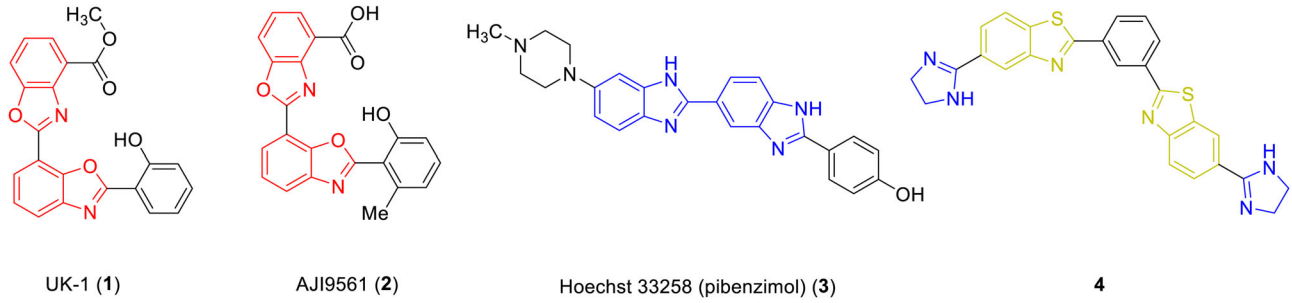

Figure 1. Structure of the previously synthesized di-heterocyclic benzazole derivatives with antiproliferative activity.

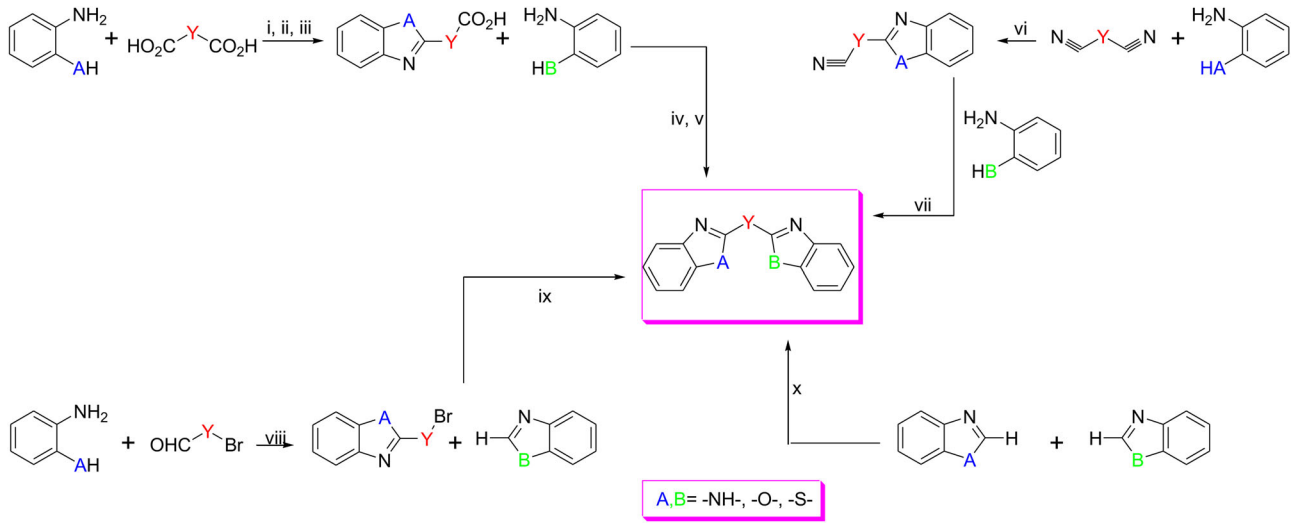

Scheme 1. Some synthesis methods of di-heterocyclic benzazoles. Reaction conditions: (*i*) [A = NH, Y = $-CH_2SCH_2-$], 6 M HCl, reflux, 72 h (*ii*) NH_3 (pH-9) (*iii*) concentrated HCl (to pH = 7) (*iv*) [B = O, S], 4 M HCl, refluxed 17 h, NH_3 (pH = 9) (*v*) recrystallized from ethanol/charcoal and water (*vi*) [A = S, Y = $-CH_2-$] *n*-BuLi (*vii*) [B = NH, O], polyphosphoric acid, 180 °C (*viii*) [A = –S–, meta disubstituted –Ar–], DMSO, 180 °C (*ix*) [B; NMe, –O–], $PdCl(C_3H_5)dppb$], Cs_2CO_3, DMF, 150 °C (*x*) [A, B = NH, S, O Y = without linker] Co/Cu.

these against different cancer cell lines (Figure 1) (Ueki et al., 1993; Sato et al., 2001). Hoechst 33258 (**3**) is a benzimidazole di-heterocyclic compound that has some antitumor activity against murine leukemias and P388 tumors; however, a phase II trial against pancreatic cancer was abandoned on account of toxicity (Jenkins, 2000; Singh et al., 1992). Racané *et al.* illustrated that imidazole-substituted bis-benzothiazole derivative (**4**) acts as an antiproliferative agent (Figure 1) (Racané et al., 2012).

A cyclocondensation reaction of two equivalents of 1,2-phenylenediamine/2-aminophenol/2-mercaptoaniline with one equivalent of bisimidate, malonic dinitrile, or dicarboxylic acid is well-known for the synthesis of symmetrical bisbenzazole derivatives (Dauer et al., 2016; Elagab & Alt, 2015; Kretsch et al., 2019;). Although, some methods are used for the preparation of symmetrical bis-benzazole derivatives, there are few methods in the literature for use in the synthesis of symmetrical di-heterocyclic derivatives.

In the synthesis of di-heterocyclic compounds from benzazole derivatives, there are difficulties in selectivity between self-binding and cross-linking products (Monguchi et al., 2010). Regardless of these challenges, different strategies have been used to obtain unsymmetrical cross-coupled di-heterocyclic benzazole products, as shown in Scheme 1. Dang *et al.* reported examples of di-heterocyclic compounds which were prepared by a two-step procedure using $PdCl(C_3H_5)dppb$ (dppb:1,4-Bis(diphenylphosphino)butane) and cesium carbonate (Cs_2CO_3) as catalysts (Dang et al., 2016). Li *et al.* discovered that cobalt and copper can be co-catalyzed in cross-dehydrogenative coupling reactions of benzazoles using air as an oxidant which leads to the formation of symmetrical and unsymmetrical di-heterocyclic compounds (Li et al., 2019). In the literature, reported different reaction conditions to obtain di-heterocyclic compounds of benzimidazole and benzothiazole using a Cu(II)-containing nano silica triazine dendrimer (Cu(II)-TD@nSiO2) and rhodium as the catalyst (Nasr-Esfahani et al., 2013; Wu et al., 2017). Dauer *et al.* treated aniline derivatives with nitrile derivatives in a two-step procedure for the synthesis of di-heterocyclic compounds (Dauer et al., 2017). But, Matthews *et al.* faced difficulties to obtain unsymmetrical compounds using concentrated hydrochloric acid condensation reaction (Matthews et al., 1996).

Nevertheless, these strategies have deficiencies because hazardous and expensive ligands and catalysts are employed with low yields. The main difficulties in this area are that simple, economical and accessible strategies have not been

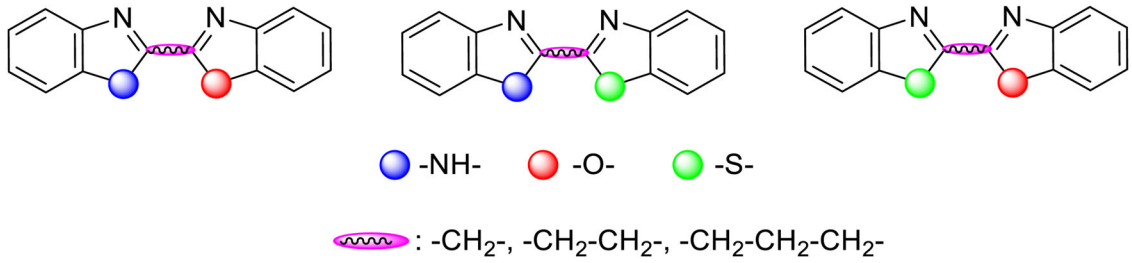

Figure 2. The molecular design strategy for the synthesis of novel di-heterocyclic benzazole derivatives bearing aliphatic linkers.

developed for the synthesis of high-yield and asymmetric cross-linked di-heterocyclic products.

The strong to excellent antitumor potential of di-benzazole derivatives has fascinated our group. Thus, we synthesized some di-heterocyclic compounds with different aliphatic linkers between heterocyclic rings (Figure 2) and evaluated their antiproliferative activity in human hepatocellular (HepG2), human renal cancer (A498), human lung adenocarcinoma epithelial (A549), and human cervical cancer (HeLa) cell lines. Additionally, we tested the role of linker groups between benzazole rings in regard to selectivity and antiproliferative activity.

It is important that the prediction of ADME properties of all the compounds, molecular reactivity analyses, molecular electrostatic potential (MEP) analysis, and molecular docking studies were also performed.

2. Material and methods

2.1. DFT/B3LYP calculations

The 3D structures of the synthesized compounds were drawn with Chem3D and the molecular mechanics MM2 method was used in the same program to determine the lowest energy conformations of each molecule. Compounds are optimized using Density Functional Theory (DFT) calculations. Theoretical calculations of all synthesized compounds were carried out with the Gaussian 09 W program. The calculations were done using the (DFT)/B3LYP method, 6-311 G (d, p) base set for H, C, N, O, S atoms, *HOMO* (highest occupied molecular orbital), *LUMO* (lowest unoccupied molecular orbitals), *HOMO-LUMO* energy gap (Egap). Electron affinity energy ($EA = -E_{LUMO}$), Ionization potential energy ($IP = -E_{HOMO}$) and molecular electrostatic potential (MEP) analysis of the optimized structures were also calculated with this program and method. Visualization of the results was done through GaussView 5.0.8.

2.2. ADMET properties

One of the most important problems that the drug did not develop the molecule is that the compounds do not have good pharmacokinetic properties. Although many synthesized compounds may have high activity, they cannot reach clinical use due to some pharmacokinetic properties. In addition, the compounds have various toxic effects makes it difficult for these compounds to be drug molecules. Therefore, determining ADMET properties before synthesizing drug candidate molecules is very important. In this study, ADMET properties of the compounds were determined using QikProp (Maestro 11.8) PRE-ADMET and DATAWARRIOR 4.07.02 softwares.

2.3. QSAR analysis

QSAR studies have been performed on the HepG2 cell line where the compounds have the best activity. As a result of DFT calculations, various quantum-chemical descriptors (*HOMO*, *LUMO*, total dipole moment etc.) were obtained. In addition, physicochemical parameters of the compounds were determined by using QikProp (Maestro 11.8) software. Correlation analysis was carried out to determine the molecular descriptors associated with the antiproliferative activities of the compounds. In order to develop the optimal QSAR equation, molecular descriptors with higher correlation to activity were determined for multiple linear regression analysis. Then, the 'leave-one-out' (*LOO*) cross-validation method, which is one of the most frequently used methods to edit the QSAR equation, was used. As a result of linear regression analysis, R^2 (square of correlation coefficient of regression), R^2_A (is the square of adjusted correlation coefficient), r (root-mean-square deviation), Sreg (standard deviation of regression), F (Fisher's F value) q^2 (correlation coefficient) and p (p value using the F statistics) were calculated.

2.4. Molecular docking

All molecular docking studies were performed with Maestro 11.8 (Schrödinger, LLC, NY). In these studies, HepG2 was performed, where the compounds were the most active and the specificity values were highest. For these cell lines, 2NNI pdb coded crystal structures of the target proteins were obtained from the protein data bank (www.rscb.org/). Solvent molecules, ligands and segments in crystal structures have been deleted, hydrogens have been added, charges have been assigned, polar hydrogens have been removed using the software Prime (Schrödinger, LLC, NY), Impact (Schrödinger, LLC, NY), Epik (Schrödinger, LLC, NY) and Propka. Molecules were prepared and minimized with LigPrep (Maestro 11.8) software. Grid maps of the active regions of proteins were created using Maestro's receptor grid generation panel and the remaining ligands were docked to these maps 70 times

5; A = -NH-
6; A = -O-
13; A = -S-

7; n = 1
14; n = 2
15; n = 3

12; A = -NH-, B = -O-, n = 1
23; A = -O-, B = -S-, n = 1
24; A = -S-, B = -NH-, n = 1
25; A = -NH-, B = -O-, n = 2
26; A = -O-, B = -S-, n = 2
27; A = -S-, B = -NH-, n = 2
38; A = -NH-, B = -O-, n = 3
29; A = -O-, B = -S-, n = 3
30; A = -S-, B = -NH-, n = 3

Scheme 2. Synthesis of di-heterocyclic benzazole derivatives (**12**, **23-30**).

in extra precision (XP) mode using Glide (Schrödinger, LLC, NY) software.

3. Experimental

3.1. Chemistry

General Commercial grade reagents and solvents were used without further purification. The purity of all compounds was judged by TLC analysis (single-spot/two-solvent systems) using a UV lamp. Melting points were measured with Gallenkamp melting point devices. ^{1}H NMR and ^{13}C NMR spectra were taken on 400 and 100 MHz spectrometer with tetramethyl silane (TMS) as an internal standard, and chemical shifts were recorded in ppm values. The IR spectra were obtained on Perkin Elmer Spectrum One FT-IR spectrometer. Elemental analysis results were obtained on a Leco CHNS-932 instrument.

3.1.1. General procedure for the synthesis of (12, 23-30)

A mixture of aniline derivatives (**5, 6, 13**) (1 eq) and the corresponding dicarboxylic acid derivatives (**7, 14, 15**) (1 eq) were heated for a period of 6–8 h in PPA at 120 °C then the other aniline derivatives (**5, 6, 13**) (1 eq) were added to the reaction mixture and the mixture was stirred additionally for 12–14 h at 180 °C. The reaction mixture was poured onto ice water and neutralized by mixing with 5 M NaOH till slightly basic pH (8–9) to get the precipitate. The resulting precipitate was filtered off and washed with cold water. Recrystallized with a suitable solvent. The resulting crystalline compounds were filtered and the vacuumed product was dried (Scheme 2).

3.1.2. 2-((1H-benzimidazol-2-yl)methyl)benzoxazole (12)

Red powder, yield 72%. **mp** = 180 °C; **IR** (KBr, cm^{-1}) ν_{max} 3400, 3029, 2973, 1653, 1523, 1449, 843, 762; **^{1}H NMR** (400 MHz, $CDCl_3$) δ 11.11 (s, 1H, NH), 8.02 (d, J = 8.12 Hz, 1H, Ar–H), 7.81–7.69 (m, 2H, Ar-H), 7.52 (t, J = 7.72 Hz, 1H, Ar–H), 7.39 (t, J = 7.63 Hz, 2H, Ar–H), 7.26–7.22 (m, 2H, Ar–H), 4.76 (s, 2H, –CH_2); **^{13}C NMR** (100 MHz, CD_3OD) δ 155.3, 153.4, 152.8, 139.0, 138.97, 138.92, 127.6, 117.4, 117.2, 117.0, 65.7; **Anal. calcd** for $C_{15}H_{11}N_3O$: C, 72.28; H, 4.45; N, 16.86; O, 6.42; Found: C, 72.10; H, 4.37; N, 17.05.

3.1.3. 2-(Benzothiazol-2-ylmethyl)benzoxazole (23)

The above procedure was followed to yield **23**. The ^{1}H NMR and ^{13}C NMR spectra are in agreement with reported data (Dauer et al., 2017).

3.1.4. 2-((1H-benzimidazol-2-yl)methyl)benzothiazole (24)

The above procedure was followed to yield **24**. The ^{1}H NMR and ^{13}C NMR spectra are in agreement with reported data (Chuiguk & Fedotov, 1981).

3.1.5. 2-(2-(1H-benzimidazol-2-yl)ethyl)benzoxazole (25)

Light brown powder, yield 73%. **mp** = 160 °C; **IR** (KBr, cm^{-1}) ν_{max} 3453, 3058, 2930, 1569, 1459, 831, 783; **^{1}H NMR** (400 MHz, $CDCl_3$) δ 7.47 (dd, J = 3.16, 5.96 Hz, 2H, Ar–H), 7.18–7.13 (m, 4H, Ar–H), 7.01 (d, J = 8.39 Hz, 2H, Ar–H), 3.14–3.07 (m, 4H, –CH_2); **^{13}C NMR** (100 MHz, CD_3OD) δ 157.6, 156.3, 133.1, 133.0, 131.0, 130.4, 130.3, 127.9, 116.6, 116.0, 114.7, 33.4, 30.2; **Anal. calcd** for $C_{16}H_{13}N_3O$: C, 72.99; H, 4.98; N, 15.96; O, 6.08; Found: C, 72.83; H, 4.89; N, 16.03.

3.1.6. 2-(2-(Benzothiazol-2-yl)ethyl)benzoxazole (26)

Red powder, yield 71%. **mp** = 194 °C; **IR** (KBr, cm^{-1}) ν_{max} 3053, 2925, 1518, 1427, 1144, 833, 732; **^{1}H NMR** (400 MHz, DMSO-d_6) δ 7.99 (t, J = 7.20 Hz, 1H, Ar–H), 7.83 (d, J = 7.95 Hz, 1H, Ar–H), 7.69 (dd, J = 3.51, 9.35 Hz, 1H, Ar–H), 7.54–7.40 (m, 2H, Ar–H), 7.33–7.28 (m, 3H, Ar–H), 3.80–3.71 (m, 2H, –CH_2), 3.62–3.54 (m, 2H, –CH_2); **^{13}C NMR** (100 MHz, DMSO-d_6) δ 162.1, 159.7, 156.8, 136.2, 135.5, 130.1, 130.0, 125.3, 115.7, 115.2, 115.0, 31.8, 29.6; **Anal. calcd** for $C_{16}H_{12}N_2OS$: C, 68.55; H, 4.31; N, 9.99; O, 5.71; S, 11.44; Found: C, 68.66; H, 4.08; N, 10.05; S, 11.59.

3.1.7. 2-(2-(1H-benzimidazol-2-yl)ethyl)benzothiazole (27)

Light brown crystalline, yield 75%. **mp** = 198 °C; **IR** (KBr, cm^{-1}) ν_{max} 3300, 3016, 2904, 1514, 817, 624; **^{1}H NMR** (400 MHz, DMSO-d_6) δ 7.89 (d, J = 1.66 Hz, 1H, Ar–H), 7.80 (d, J = 8.77 Hz, 1H, Ar–H), 7.55 (dd, J = 1.98, 8.74 Hz, 1H, Ar–H), 7.35–7.27 (m, 4H, Ar–H), 7.25–7.21 (m, 1H, Ar–H), 3.46 (d, J = 7.76 Hz, 2H, –CH_2), 3.26 (d, J = 7.82 Hz, 2H, –CH_2); **^{13}C NMR** (100 MHz, DMSO-d_6) δ 157.1, 139.7, 130.7, 130.2, 130.1, 128.3, 128.2, 123.6, 115.8, 32.2, 30.0; **Anal. calcd**

for$C_{16}H_{13}N_3S$: C, 68.79; H, 4.69; N, 15.04; S, 11.48; Found: C, 68.65; H, 4.75; N, 14.97; S, 11.59.

3.1.8. 2-(3-(1H-benzimidazol-2-yl)propyl)benzoxazole (28)

White powder, yield 78%. **mp** = 201 °C; **IR** (KBr, cm^{-1}) ν_{max} 3407, 3245, 3063, 2954, 1523, 1414, 840, 732; **^{1}H NMR** (400 MHz, $CDCl_3$) δ 9.96 (s, 1H, N), 7.70–7.49 (m, 2H, Ar–H), 7.29 (dd, J = 3.25, 5.99 Hz, 2H, Ar–H), 7.13–6.85 (m, 4H, Ar–H), 3.11–3.03 (m, 2H, $-CH_2$), 2.59–2.51 (m, 2H, $-CH_2$), 2.28–2.18 (m, 2H, $-CH_2$); **^{13}C NMR** (100 MHz, $CDCl_3$) δ 165.5, 151.1, 138.7, 135.1, 125.4, 118.9, 110.6, 27.8, 23.7, 21.7; **Anal. calcd** for $C_{17}H_{15}N_3O$: C, 73.63; H, 5.45; N, 15.15; O, 5.77; Found: C, 73.75; H, 5.38; N, 15.22.

3.1.9. 2-(3-(Benzothiazol-2-yl)propyl)benzoxazole (29)

Beige powder; yield 74%. **mp** = 190 °C; **IR** (KBr, cm^{-1}) ν_{max} 3049, 2975, 1571, 1455, 836, 747; **^{1}H NMR** (400 MHz, DMSO-d_6) δ 7.99–7.28 (m, 8H, Ar–H), 3.32–3.26 (m, 2H, $-CH_2$), 3.16–3.09 (m, 2H, $-CH_2$), 2.55–2.47 (m, 2H, $-CH_2$); **^{13}C NMR** (100 MHz, DMSO-d_6) δ 157.5, 156.1, 156.0, 137.7, 135.0, 134.9, 128.9, 128.1, 125.6, 121.3, 32.8, 30.4, 20.6; **Anal. calcd** for $C_{17}H_{14}N_2OS$: C, 69.36; H, 4.79; N, 9.52; O, 5.43; S, 10.89; Found: C, 69.25; H, 4.68; N, 9.59; S, 10.75.

3.1.10. 2-(3-(1H-benzimidazol-2-yl)propyl)benzothiazole (30)

Yellow powder, yield 76%. **mp** = 189 °C; **IR** (KBr, cm^{-1}) ν_{max} 3383, 2981, 2918, 1603, 1511, 1232, 801, 752; **^{1}H NMR** (400 MHz, d_6-DMSO) δ 8.06 (d, J = 7.90 Hz, 1H, Ar–H), 7.95 (d, J = 8.10 Hz, 1H, Ar–H), 7.51–7.47 (m, 3H, Ar–H), 7.41 (t, J = 7.56 Hz, 2H, Ar–H), 7.14 (d, J = 3.11 Hz, 1H, Ar–H), 3.24 (t, J = 7.47 Hz, 2H, $-CH_2$), 2.99 (t, J = 7.47 Hz, 2H, $-CH_2$), 2.39–2.31 (m, 2H, $-CH_2$); **^{13}C NMR** (100 MHz, DMSO-d6) δ 157.4, 138.0, 135.0, 129.1, 128.9, 128.0, 126.5, 123.5, 32.6, 30.4, 20.6; **Anal. calcd** for $C_{17}H_{15}N_3S$: C, 69.60; H, 5.15; N, 14.32; S, 10.93; Found: C, 69.51; H, 5.28; N, 14.41; S, 10.87.

3.2. Biological studies

3.2.1. Antiproliferative activity

The synthesized compounds were tested *in vitro* for their cytotoxic properties against tumor cell lines panel by using MTT assay Mosmann's method. The MTT assay is based on the reduction of the soluble MTT (0.5 mg mL–1.100 μL), into a blue-purple formazan product mainly by mitochondrial reductase activity inside living cells (Mosdam, 1983). The cells used in cytotoxicity assay were cultured in RPMI 1640 medium supplemented with 10% fetal calf serum, Penicillin, and streptomycin at 37 °C and humidified at 5% CO_2. Briefly cells were placed on 96-well plates at 100 mL total volume with density of 1–2.5 × 10^4 cells per mL and were allowed to adhere for 24 h before treatment with tested drugs in DMSO solution (10-5.10-6.10-7 mol L^{-1} final concentration). Triplicate wells were treated with media and agents. Cell viability was assayed after 96 h of continuous drug exposure with a tetrazolium compound. The supernant medium was removed and 150 mL of DMSO solution was added to each well. The plates were gently agitated using mechanical plate mixer until the color reaction was uniform and the OD570 was determined using micro plate reader. The 50% inhibitory concentration (IC_{50}) was defined as the concentration that reduced the absorbance of the untreated wells by 50% of vehicle in the MTT assay.

The cell viability was expressed as percentage of the viable cells in each sample with respect to the control wells. Three independent experiments in triplicates were done for the determination of the growth inhibition of each compound. The IC_{50} values were calculated from concentration-response curves using the SPSS (SPSS. Inc. Chicago) Software.

4. Results and discussion

4.1. Chemistry

A synthetic strategy was developed for the formation of di-heterocyclic compounds. The main framework was a bis-benzazole compound in which the two aromatic ring structures are different. In the first method to optimize the synthesis conditions of unsymmetrical cross-coupled di-heterocyclic derivatives, 1,2-phenylenediamine (**5**) (1 eq), 2-aminophenol (**6**) (1 eq) and malonic acid (**7**) (1 eq) in the presence of polyphosphoric acid (PPA) were reacted at 180 °C for 14 h according to previously reported methodology (Chhonker et al., 2009; Elagab & Alt, 2015; Peng et al., 2016; Sun et al., 2018). A mixture of 2-(1*H*-benzimidazol-2-yl)acetic acid (**8**), 2-(benzoxazol-2-yl)acetic acid (**9**), bis(benzoxazol-2-yl)methane (**10**), bis(1*H*-benzimidazol-2-yl)methane (**11**), and 2-((1*H*-benzimidazol-2-yl)methyl)benzoxazole (**12**) at 7%, 5%, 18%, 20% and 12% yields, respectively was obtained (Route A). In the second method, the reaction of 1,2-phenylenediamine (**5**) (1 eq) and malonic acid (**7**) (1 eq) in the presence of PPA at 180 °C was carried out for 12–14 h and bis(1*H*-benzimidazol-2-yl)methane (**11**) and 2-(1*H*-benzimidazol-2-yl)acetic acid (**8**) were obtained at 30% and 36% yields, respectively (Route B). The last reaction method which was carried out at 120 °C in PPA produced 2-(1*H*-benzimidazol-2-yl)acetic acid (**8**) at a good yield of 72% (Route C) (Scheme 3).

After some preliminary experiments the best yield of the desired di-benzazole derivatives (**12**, **23-30**) was obtained when the dicarboxylic acid derivatives (**7, 14, 15**) (1 eq) were treated with aniline derivatives (**5, 6, 13**) (1 eq) at 120 °C in 6–8 h without isolation. Then, the corresponding aniline derivatives (**13, 5, 6**) (1 eq) were added to the reaction mixture in 12–14 h at 180 °C (Route C and D). This method was an ideal strategy, thereby greatly reducing the number of reaction steps and increasing the reaction yield (Scheme 3).

The optimized reaction conditions were then applied to the synthesis of a series of unsymmetrical cross-coupled di-heterocyclic derivatives (**12**, **23-30**) (Scheme 3).

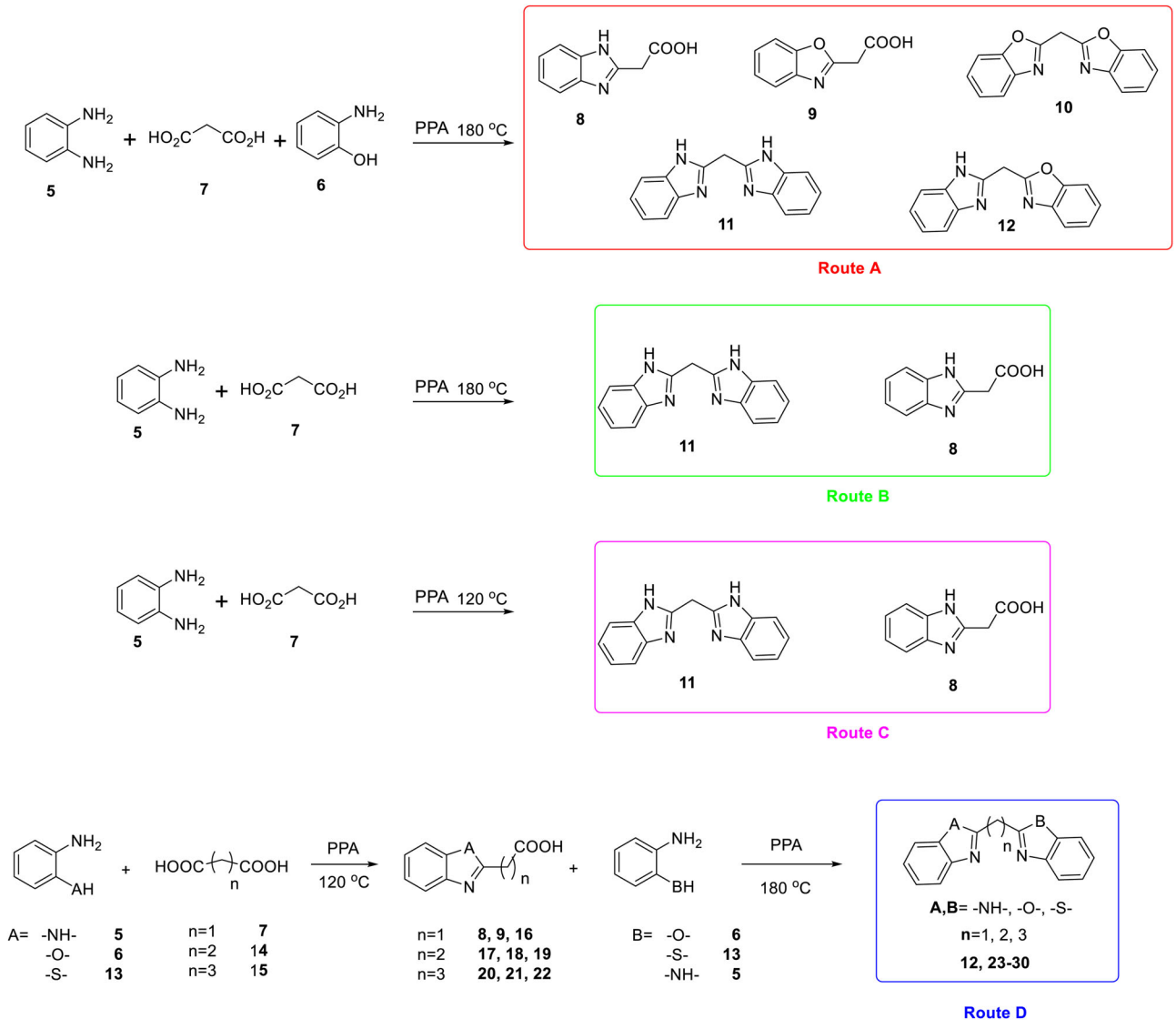

Scheme 3. Optimization of reaction conditions.

4.2. Antiproliferative activity

All synthesized compounds (**12**, **23–30**) were evaluated for their *in vitro* antiproliferative activity against four human cancer cell lines by comparing the results with the standard antiproliferative drug methotrexate. The *in vitro* antiproliferative screening of the compounds against HepG2, A498, A549, and HeLa was performed using the MTT assay (Mosdam, 1983). The results of the *in vitro* antiproliferative activities are summarized in Table 1. The selectivity of these compounds towards cancerous cells was evaluated against Vero (African green monkey kidney epithelial) cells to study their cytotoxic nature.

The synthesized compounds displayed good antiproliferative activities against the tested human cancer cell lines. Diheterocyclic compounds with benzoxazole and benzothiazole rings were observed as the most potent antiproliferative agents against the tested cancer cell lines. Among the synthesized compounds benzothiazole derivatives (**23** and **27**) showed promising antiproliferative activity against all the tested cancer cell lines. Compounds with benzoxazole and benzothiazole moieties (**23**, **26,** and **29**) were the most potent antiproliferative agents against HepG2 and HeLa cancer cell lines with IC_{50} values of 7.81 μM and 15.63 μM. respectively. Compound **23** was two times more selective towards HepG2 (IC_{50}. 7.81 μM) than towards Vero. Similarly, compound **27** was two times more selective towards the HepG2 cancer cell line than the Vero cell line with IC_{50} values of 15.63 μM and 31.25 μM, respectively (Table 1).

Among the synthesized derivatives compound **23** showed good selectivity and antiproliferative activity with IC_{50} values of 7.81 and 15.63 μM against A498 and Vero cell lines, respectively; thus compound **23** was two times more selective towards the A498 cancer cell line than towards the Vero line. Additionally, compound **27** showed good selectivity towards A498. with an IC_{50} value of 15.63 μM.

Compounds with a methylene linker (**23** and **24**) were good antiproliferative agents against the A549 cancer cell line with an IC_{50} value of 15.63 μM and the selectivity was observed with benzoxazole and benzothiazole rings bearing

Table 1. Antiproliferative activity of the synthesized benzazole derivatives.

Compound No	Vero	HepG2	A498	A549	HeLa	Specificity			
			IC_{50} (μM)			HepG2	A498	A549	HeLa
12	31.25 ± 1.28	125 ± 4.52	62.5 ± 1.85	125 ± 2.42	62.5 ± 3.02	0.25	0.5	0.25	0.5
23	15.63 ± 1.24	7.81 ± 1.93	7.81 ± 1.04	15.63 ± 1.89	15.63 ± 1.12	2.00	2.00	1.00	1.00
24	3.91 ± 1.58	15.61 ± 2.54	15.63 ± 0.56	15.63 ± 2.36	31.25 ± 1.42	0.25	0.25	0.25	0.12
25	7.81 ± 0.67	15.3 ± 0.98	31.25 ± 1.96	31.25 ± 2.35	31.25 ± 2.13	0.5	0.25	0.25	0.25
26	3.91 ± 1.61	7.81 ± 1.05	31.25 ± 0.99	31.25 ± 1.37	15.63 ± 1.93	0.5	0.12	0.12	0.25
27	31.25 ± 0.34	15.63 ± 2.28	15.63 ± 1.58	31.25 ± 2.42	31.25 ± 1.56	2.00	2.00	1.00	1.00
28	7.81 ± 1.10	15.63 ± 3.36	15.63 ± 0.75	31.25 ± 1.67	15.63 ± 2.65	0.5	0.5	0.25	0.5
29	3.91 ± 1.86	7.81 ± 1.24	15.63 ± 1.08	31.25 ± 0.72	15.63 ± 0.47	0.5	0.25	0.12	0.25
30	7.81 ± 2.12	15.63 ± 2.04	31.25 ± 2.28	31.25 ± 2.89	15.63 ± 1.62	0.5	0.25	0.25	0.5
MTX	0.030 ± 0.41	0.041 ± 0.12	0.016 ± 0.28	0.025 ± 0.53	0.022 ± 0.36	0.73	1.87	1.20	1.36

Table 2. Calculated quantum-chemical descriptors.

Compounds	*HOMO*	*LUMO*	Gap (ΔE)	IP($-E_{HOMO}$)	EA ($-E_{LUMO}$)
12	−6.07739	−1.30941	−4.76798	6.07739	1.30941
23	−6.63768	−1.35894	−5.27874	6.63768	1.35894
24	−6.10107	−1.50697	−4.5941	6.10107	1.50697
25	−6.14297	−1.09471	−5.04826	6.14297	1.09471
26	−6.59659	−1.17063	−5.42595	6.59659	1.17063
27	−6.19794	−1.28002	−4.91792	6.19794	1.28002
28	−6.07848	−1.05607	−5.02241	6.07848	1.05607
29	−6.56203	−1.10315	−5.45888	6.56203	1.10315
30	−6.15059	−1.24492	−4.90567	6.15059	1.24492

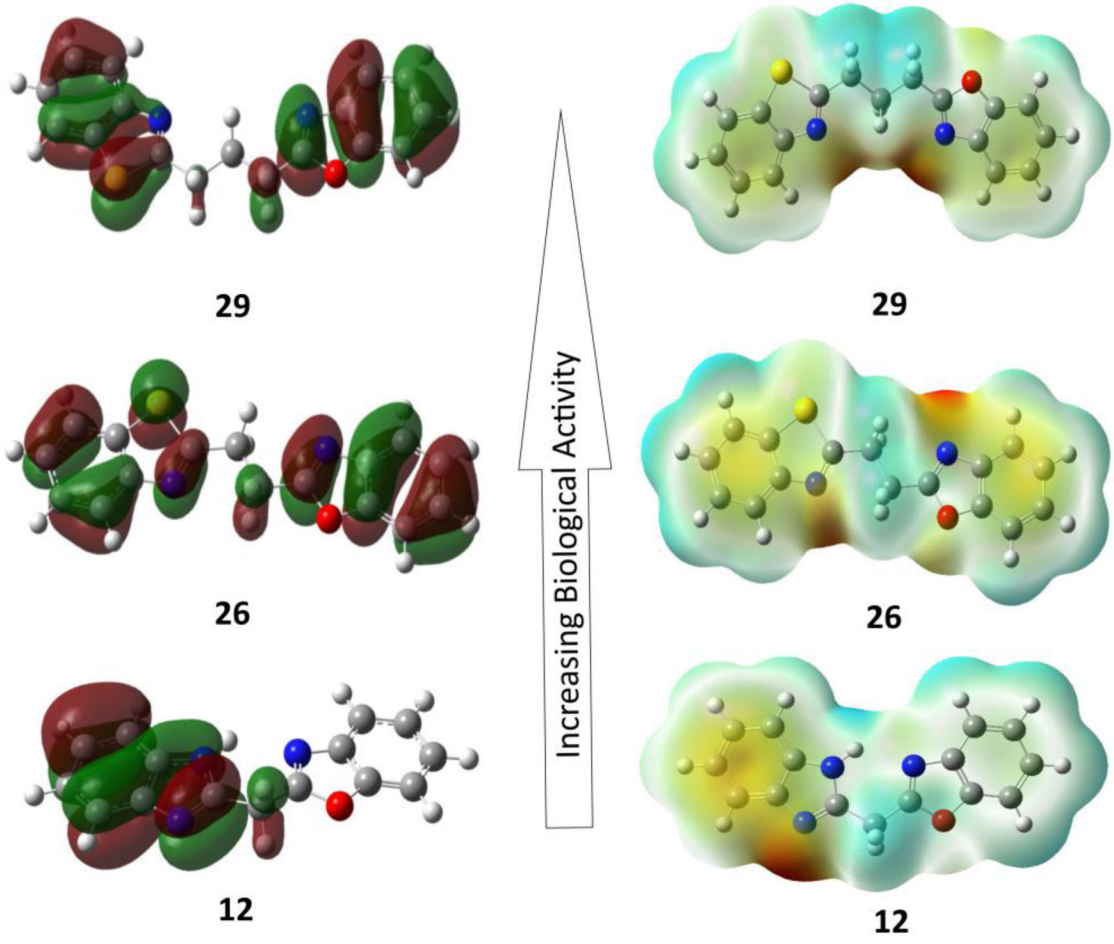

Figure 3. Molecular electrostatic potential and *HOMO* orbital of highest. Moderate and excessive biological activity compounds **12**. **26** and **29** by DFT/B3LYP calculations.

derivative **23**. Compounds with a propylene linker (**28**, **29,** and **30**) were screened to determine their toxicity against the normal cell line (Vero) and they were more toxic to human cell lines than the positive control compound methotrexate (Table 1).

4.3. Molecular reactivity analyses

Molecular geometries of all molecular structures were fully optimized using DFT/B3LYP. From the results of the DFT calculations the quantum-chemical descriptors were obtained for the model building as the energy levels of the molecular orbital order *HOMO* (highest occupied molecular orbital) and *LUMO* (lowest unoccupied molecular orbital) for molecules give information on the possible electronic transition. The *HOMO* and *LUMO* also indicate the electrophilic and nucleophilic attraction in molecule. The energy range created by *HOMO* and *LUMO* is an indicator of the chemical stability of the molecule and can be a critical parameter to determine the electrical transfer properties of the compounds (Erol et al., 2020; Reddy et al., 2016). The E_{HOMO}-E_{LUMO} (Gap) is the most important parameter for the chemical reactivity. Quantum-chemical descriptors (*HOMO, LUMO*, Gap, EA) of the molecules are given in Table 2. The likelihood and selectivity of the reactions depend on the energies and symmetries of these leading orbitals.

A correlation was established between the calculated quantum-mechanical parameters and the activities of all synthesized compounds. In this correlation analysis, *HOMO* values were found to be in high relationship with activity.

4.4. Geometry optimization and MEP analysis

Molecular docking studies showed that benzazole groups were effective in the antiproliferative activities and compounds interact with residues in the active region of the receptor through these groups. In QSAR studies, *HOMO* energies were found to be closely related to activity. Once *HUMO* energy related to biological activity need to investigate the other aspect like location of these orbitals on the molecule (Figure 3). Such investigation of electronic densities revealed the location of particular part in a compound influenced the biological activity. It can be seen that *HOMO* orbitals settle on molecules **12, 26** and **29**, especially on benzazole groups (Figure 3). Although *HOMO* orbitals are located on only one benzazole ring in compound **12**, **26** and **29** appear in both ring systems on the bisbenzazole structure of these orbitals. Therefore, depending on the localization of *HOMO* orbital bisbenzazole-derived compounds have theoretically proposed to have different biological activities.

4.5. In silico ADMET prediction

In silico ADMET studies of the compounds were conducted to determine various physicochemical properties, inappropriate pharmacokinetic properties and possible toxicities of molecules. In silico ADMET and toxicological screening systems can provide an opportunity to predict performance

Table 3. Some predicted toxicological, ADME, and drug-like properties.

Parameters	Compound 7	Compound 8	Compound 9	Compound 10	Compound 11	Compound 12	Compound 13	Compound 14	Compound 15
Toxicological									
Irritant[a]	None	None	None	None	None	None	None	None	None
Reproductive effects[a]	None	None	None	None	None	None	None	None	None
Carcinogenic[a]	None	None	None	None	None	None	None	None	None
Mutagenic[a]	None	None	None	None	None	None	None	None	None
hERG inhibition[b]	Medium risk	Medium risk	Medium risk	Medium risk	Medium risk	Medium risk	Medium risk	Medium risk	Medium risk
CYP450 inhibition[b]	2C19.2C9.3A4	2C19.2C9.3A4	2C19.2C9.3A4	2C19.2C9.3A4	2C19.2C9.3A4	2C19.2C9.3A4	2C19.2C9.3A4	2C19.2C9.3A4	2C19.2C9.3A4
ADME									
Blood–brain barrier	High absorption	High absorption	High absorption	High absorption	High absorption	High absorption	High absorption	Low absorption	High absorption
Human intestinal absorption[b]	Well absorbed	Well absorbed	Well absorbed	Well absorbed	Well absorbed	Well absorbed	Well absorbed	Well absorbed	Well absorbed
Plasma protein binding[b]	Strongly bound	Strongly bound	Weakly bound	Weakly bound	Strongly bound	Strongly bound	Weakly bound	Strongly bound	Weakly bound
Caco2 permeability[b]	Middle permeability	Middle permeability	Middle permeability	Middle permeability	Middle permeability	Middle permeability	Middle permeability	Middle permeability	Middle permeability
Drug-like									
Drug-likeness score[a]	0.228	1.034	1.73	−0.821	−0.015	0.680	−2.701	−1.895	−1.2
CMC-like rule[b]	Qualified	Qualified	Qualified	Qualified	Qualified	Qualified	Qualified	Qualified	Qualified
Lead-like rule[b]	Violated	Violated	Violated	Violated	Violated	Violated	Violated	Violated	Violated
Rule of five[b]	Suitable	Suitable	Suitable	Suitable	Suitable	Suitable	Suitable	Suitable	Suitable
WDI-like rule[b]	Suitable	Suitable	Suitable	Suitable	Suitable	Suitable	Suitable	Suitable	Suitable

[a]Determined by datawarrior v4.07.02.
[b]Determined by pre-admet. (https://preadmet.bmdrc.kr).

in vivo. Estimates of ADMET properties of all synthesized compounds were performed with PRE - ADMET and DATAWARRIOR 4.07.02 software. The software evaluated drug candidates' ADMET profiles according to CMC-like, lead-like, Lipinski's rule of five, and WDI-like rules.

Toxicological, ADME, and Drug-like values were shown in Table 3. Scores were observed to be within the range of traded drugs. When the toxicological parameters (mutagenic, carcinogenic, irritant, reproduction effects) were examined, it was seen that all the compounds did not have an estimated toxicity. Also, it is important points to know about these principle predictors for the compounds were determined using QikProp (Maestro 11.8) (details are provided in the supplementary content of Table S1).

4.6. QSAR analyses

In QSAR studies, the relationship between the physicochemical, electronic and structural properties and biological activities of chemical compounds are examined quantitatively by mathematical methods. In these studies, the rational design of new lead compounds is provided and data that can contribute to their development are obtained.

In this study, an optimal QSAR equation (1) containing eight compounds was obtained by multiple linear regression method with QSAR analysis.

$$\text{Log } 1/IC_{50} = -7.558 - 1.013 \text{ x } E_{HOMO} \quad (1)$$

$$n = 9;\ R^2 = 0.437;\ R^2{}_A = 0.357;\ r = 0.29;\ q^2 = 0.123$$

$$S_{reg} = 0.47;\ F = 5.444;\ p < 0.052$$

Table 4. Molecular docking scores of all compounds.

Compounds	Docking Scores for protein (2NNI)
12	−3.708
23	−5.569
24	−5.216
25	−5.247
26	−5.562
27	−5.257
28	−4.842
29	−5.914
30	−5.167
MTX	−7.336

A good QSAR model; R^2 must be > 0.7; q2 must be > 0.5; large F should be small r and p value < 0.001. It was seen that compound **12** which constitutes our QSAR equation has the largest regression deviation and is accepted as an outlier. After excluding compound **12**, an optimal QSAR model was obtained as follows and the established QSAR equation (2) appears to be statistically successful.

$$\text{Log } 1/IC_{50} = -5.033 - 0.626 \text{ x } E_{HOMO} \quad (2)$$

$$n = 8;\ R^2 = 0.972;\ R^2{}_A = 0.967;\ r = 0.0277;\ q^2 = 0.953$$

$$S_{reg} = 0.163;\ F = 212.136;\ p < 0.000001$$

The newly created equation is very successful statistically. While R^2 value in Equation (1) is 0.437. R^2 value in Equation (2) is 0.972; the q^2 value was calculated as 0.953 in Equation (2) instead of 0.123. The p value which should be less than 0.001 has decreased considerably compared to the first equation. According to Equation (2), E_{HOMO} values were found to be closely related to the antiproliferative activities of compounds with the bisbenzazole skeleton.

In this study, a correlation was made to determine a relationship between the antiproliferative activity of the compounds and the physicochemical parameters calculated. However, the correlation coefficient (r) values of these parameters were found less than 0.5 and were not evaluated.

4.7. Molecular docking

Molecular docking is a significant computer-assisted drug design method for predicting the main binding modes of a ligand with a protein of known three-dimensional structure (Sepehri et al., 2017). In order to know the possible binding studies of the di-heterocyclic compounds (**12, 23-30**) molecular interaction studies of the active anti-cancer compounds were performed against human P450 (CYP) 2C8 (CYP2C8) enzyme. CYP2C8 accounts for approximately 6–7% of the total hepatic CYP content (Achour et al., 2014). The importance of CYP2C8 causing variation in drug response via drug-drug interactions and pharmacogenetics polymorphisms has been recognized only for the last two decades. CYP2C8 participates in the metabolism of numerous drugs and some endogenous and natural compounds. It catalyzes

Table 5. Intermolecular interactions of the most active compounds (**26** and **29**) and MTX in the active region of the protein (pdb ID: 2NNI).

Compounds	Interactions Type	Protein residues	Distance in Å
26	pi-pi stacking	PHE205	4.79; 5.32
	Hydrophobic	ILE106. PHE201. PHE205. LEU208. VAL233. VAL237. ALA292. ALA296. ALA297. ILE476. VAL477	
	Polar	THR107. ASN204. ASN209. ASN236. THR240. THR301	
	Charged (+)	ARG200. ARG241	
	Charged (−)	ASP293. GLU300	
29	pi-pi stacking	PHE205	4.92; 5.38
	Hydrophobic	ILE106. LEU110. LEU208. VAL237. VAL244. VAL288. ALA292. ALA296. ALA297. ILE476. VAL477	
	Polar	THR107. ASN202. ASN204. ASN209. ASN236. THR240. THR301	
	Charged (+)	ARG200. ARG241	
MTX	pi-pi stacking	HEM	4.91; 4.92
	H-bound	ARG241	1.58
	Hydrophobic	ILE102. ILE103. LEU110. PHE205. VAL207. LEU208. VAL288. ALA292. ALA297. LEU361. LEU362. VAL366. ILE476. VAL477	
	Polar	SER103. SER114. THR107. ASN204. ASN236. THR301. THR240. LYS108	

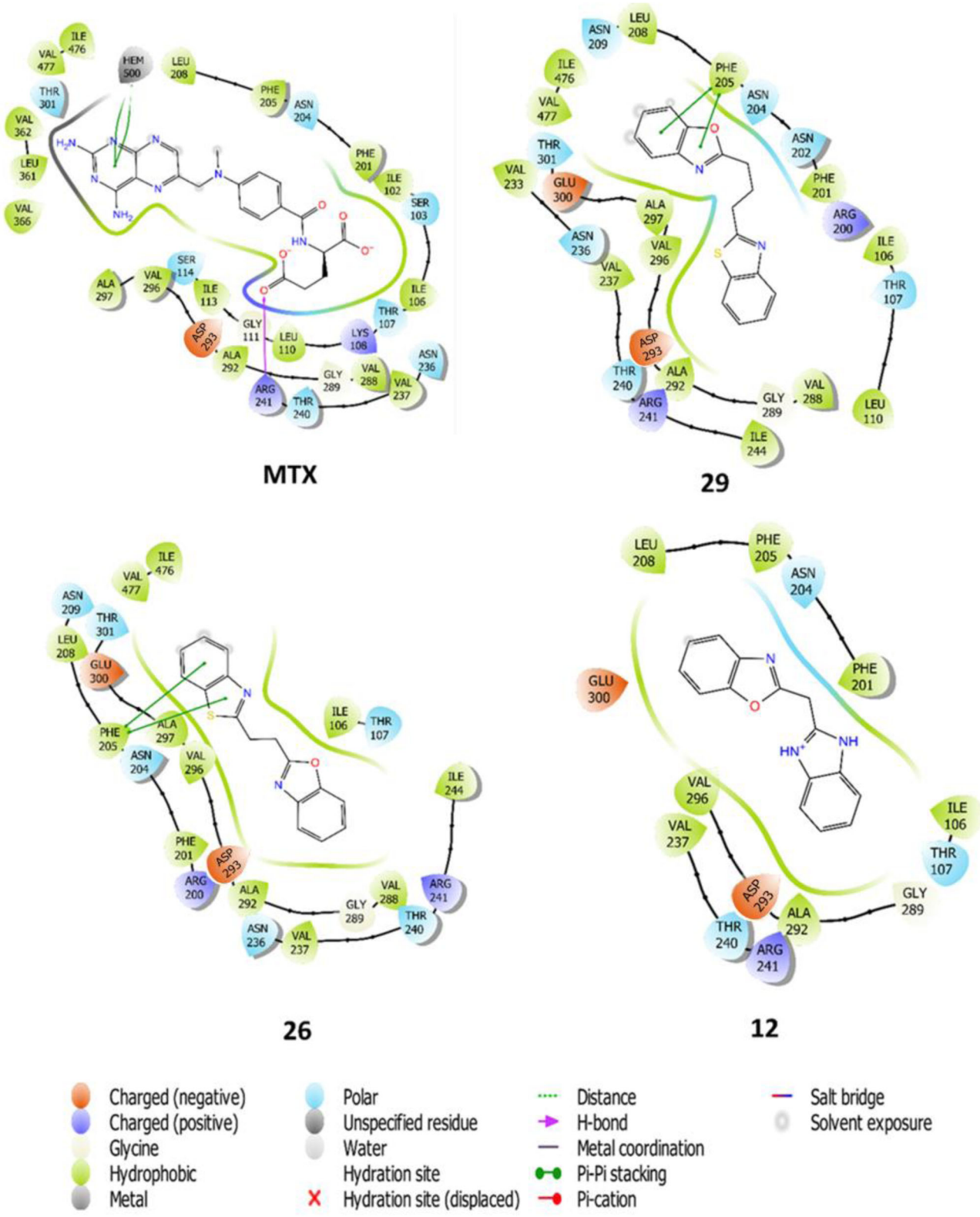

Figure 4. 2D interaction **12. 26. 29** and **MTX** with active site of protein (2NNI).

a variety of oxidative reactions, in particular hydroxylation, N-demethylations, and N-deethylations. Because of its large, sinuous active site, CYP2C8 can accommodate substrates of different sizes and structures. Typical substrate drugs of CYP2C8 include anticancer, antidiabetic, antimalarial, and lipid-lowering agents. Interestingly, some glucuronide metabolites of drugs interact with CYP2C8. The event was the onset of a broadening scientific interest in CYP2C8, promptly convincing drug regulatory authorities to acknowledge CYP2C8 as one of the major drug-metabolizing CYP enzymes.

The crystal structure of the 2NNI pdb coded CYP2C8dH protein was used in the docking studies on the HepG2 cell line. Although the reference molecule methotrexate has a

−7.336 kcal/mol docking score; the scores of the compounds **23, 26** and **29** (IC_{50} = 7.81 μM) were −5.569, −5.562 and −5.914 − 6.168 kcal/mol respectively; the scores of compounds **24, 25, 27, 28,** and **30** (IC_{50} = 15.3 − 15.63 μM) are −5.216, −5.247, −5.257, −4.842 and −5.167 kcal/mol, respectively (Table 4).

The lowest experimental activity result (IC_{50} = 125 μM) was compound **12** and the docking score was calculated as −3.708 kcal/mol. Docking study results showed that docking scores and activity results appear to be in harmony. It is seen that the methotrexate structure has the highest activity. Pi-pi stacking interaction with HEM in the active region of the protein of the pteridine ring in the methotrexate structure were hydrogen bond with ARG241; and hydrophobic polar and charged (+) interactions with various residues.

Compounds **26** and **29** have the highest activity and have been found to interact with PHE205 in the active region of the receptor, and to interact with various residues hydrophobic, polar and charged (+) (Table 5). Compound **12** with the lowest docking score was found to do no pi-pi stacking interaction and hydrogen bonding with residues. It is thought that the low docking score of compound **12** is due to the inability to fully settle in the active site and to make strong bonds with the residues (Figure 4).

5. Conclusion

In the development of potent small and active anticancer molecules an approach in which two bioactive heterocyclic scaffolds are embedded in a single molecule using an easy, simple and economical one-stage reaction strategy with good selectivity and moderate to good isolated yields of di-heterocyclic molecules can be used. However, the synthesis of di-benzazoles is not as easy as that of bis-structures. Careful examination led to the establishment of a significantly regular structure-activity relationship which indicated that the di-heterocyclic compounds with benzoxazole and benzothiazole moieties are the most potent antiproliferative agents with good selectivity against cancer cell lines.

Benzothiazole and benzoxazole rings show better anticancer activity than the benzimidazole ring. Additionally, the antiproliferative activity is higher with a methylene linker than with a propylene linker. The flexibility of two di-heterocyclic compounds should not be too high for antiproliferative activity.

In order to explain the relationship between the activity and structure of these compounds, QSAR study was performed by calculating various physicochemical parameters with various quantum-chemical descriptors and QikProp software using DFT calculations. In QSAR studies, *HOMO* values of the compounds were determined to be highly related to activity and a QSAR equation was created by multiple regression analysis method (Log $1/IC_{50} = -5.033 - 0.626E_{HOMO}$). According to the QSAR equation predicted and experimental IC_{50} values are very close to each other (Table 4). Molecular docking studies were also conducted to control the results of QSAR studies and to examine the interactions of molecules (**12, 23-30**) and MTX with the receptor. In docking studies, it was determined that the docking scores of the compounds **23-30** were between −4.842 and −5.914 kcal/mol and the compound **12** removed from the QSAR equation with the *LOO* method was −3.708 (Table 4). It was also observed that compound **7** did not make significant interactions with residues in the active region of the receptor. These results explain why the predicted IC_{50} value (16.77 μM) of compound **12** in the QSAR equation is different from the experimental IC_{50} value (125 μM) of the compound.

The results obtained by using the QSAR equation that we created to design new and higher antiproliferative molecules with a bisbenzazole skeleton can be supported by molecular docking studies. Finally, asymmetric di(benzazol-2-yl)ethanes can be regarded as promising drug leads for the development of effective anticancer drugs.

Disclosure statement

The authors have declared no conflict of interest.

Funding

We thank the Scientific and Technological Research Council of Turkey (TUBITAK Grant Number: 115S190) and Mersin University for their financial support (BAP-SBE-2018-1-TP3-2911).

References

Achour, B., Barber, J., & Rostami-Hodjegan, A. (2014). Expression of hepatic drug metabolizing cytochrome p450 enzymes and their intercorrelations: A meta-analysis. *Drug Metabolism and Disposition*, *42*(8), 1349–1356. https://doi.org/10.1124/dmd.114.058834

Aiello, S., Wells, G., Stone, E. L., Kadri, H., Bazzi, R., Bell, D. R., Stevens, M. F. G., Matthews, C. S., Bradshaw, T. D., & Westwell, A. D. (2008). Synthesis and biological properties of benzothiazole, benzoxazole, and chromen-4-one analogues of the potent antitumor agent 2-(3,4-dimethoxyphenyl)-5-fluorobenzothiazole (PMX 610, NSC 721648). *Journal of Medicinal Chemistry*, *51*(16), 5135–5139. https://doi.org/10.1021/jm800418z

Can-Eke, B., Puskullu, M. O., Buyukbingol, E., & Iscan, M. (1998). A study on the antioxidant capacities of some benzimidazoles in rat tissues. *Chemico-Biological Interactions*, *113*(1), 65–77. https://doi.org/10.1016/S0009-2797(98)00020-9

Chhonker, Y. S., Veenu, B., Hasim, S. R., Kaushik, N., Kumar, D., & Kumar, P. (2009). Synthesis and pharmacological evaluation of some new 2-phenyl benzimidazoles derivatives and their Schiff's bases. *E-Journal of Chemistry*, *6*(S1), S342–S346. https://doi.org/10.1155/2009/604203

Chuiguk, V., & Fedotov, K. (1981). Pyrido (1, 2-a) benzimidazoles and pyrido (1, 2-a)-and-(2, 1-b) benzazolium salts from diheterylmethanes and 1, 3-diketones. *Chemischer Informationsdienst*, *12*(30), 197-202. https://doi.org/10.1002/chin.198130218

Cressier, D., Prouillac, C., Hernandez, P., Amourette, C., Diserbo, M., Lion, C., & Rima, G. (2009). Synthesis, antioxidant properties and radioprotective effects of new benzothiazoles and thiadiazoles. *Bioorganic & Medicinal Chemistry*, *17*(14), 5275–5284. https://doi.org/10.1016/j.bmc.2009.05.039

Dang, T. T., Soulé, J.-F., Doucet, H., Benmensour, M. A., Boucekkine, A., Colombo, A., Dragonetti, C., Righetto, S., Jacquemin, D., Boixel, J., & Guerchais, V. (2016). Asymmetrical 1, 3-bis (heteroazolyl) benzene platinum complexes with tunable second-order non-linear optical properties. *European Journal of Inorganic Chemistry*, *2016*(29), 4774–4782. https://doi.org/10.1002/ejic.201600675

Dauer, D. R., Flügge, M., Herbst-Irmer, R., & Stalke, D. (2016). Group 13 metal complexes containing the bis-(4-methylbenzoxazol-2-yl)-methanide ligand. *Dalton Transactions (Cambridge, England: 2003)*, *45*(14), 6149–6158. https://doi.org/10.1039/C5DT03913D

Dauer, D. R., Koehne, I., Herbst-Irmer, R., & Stalke, D. (2017). From Bis (imidazol-2-yl) methanes to asymmetrically substituted bis (heterocyclo) methanides in metal coordination. *European Journal of Inorganic Chemistry*, *2017*(13), 1966–1978. https://doi.org/10.1002/ejic.201601470

Dubey, R., Shrivastava, P. K., Basniwal, P. K., Bhattacharya, S., Moorthy, N., & Narayana, S. H. (2006). 2-(4-aminophenyl) benzothiazole: A potent and selective pharmacophore with novel mechanistic action towards various tumour cell lines. *Mini Reviews in Medicinal Chemistry*, *6*(6), 633–637. https://doi.org/10.2174/138955706777435706

Elagab, H. A., & Alt, H. G. (2015). Structure–property-relationship studies with ethylene polymerization catalysts of Ti, Zr and V containing heterocyclic ligands. *Inorganica Chimica Acta*, *437*, 26–35. https://doi.org/10.1016/j.ica.2015.08.002

Erol, M., Celik, I., Temiz-Arpaci, O., Kaynak-Onurdag, F., & Okten, S. (2020). Design, synthesis, molecular docking, density functional theory and antimicrobial studies of some novel benzoxazole derivatives as structural bioisosteres of nucleotides. *Journal of Biomolecular Structure and Dynamics*, 1–12. https://doi.org/10.1080/07391102.2020.1760134

Han, X., Shen, K., Huang, G., Li, C., Mao, S., Shi, X., & Wu, H. (2018). Synthesis, structure, electrochemical properties and superoxide radical scavenging activities of two thiocyanate copper (II) complexes with different pyridyl-benzoxazole ligands. *Journal of Molecular Structure*, *1169*, 18–24. https://doi.org/10.1016/j.molstruc.2018.05.058

Himmetoglu, S., Dincer, Y., Ersoy, Y. E., Bayraktar, B., Celik, V., & Akçay, T. (2009). DNA oxidation and antioxidant status in breast cancer. *Journal of Investigative Medicine*, *57*(6), 720–723. doi.org/10.1093/jn/132.2.303 https://doi.org/10.2310/JIM.0b013e3181adfb5b

Jenkins, T. C. (2000). G-quadruplex DNA: a target for drug design. *Current Medicinal Chemistry*, *7*, 99–115. https://doi.org/10.2174/0929867003375551

Kretsch, J., Koehne, I., Lõkov, M., Leito, I., & Stalke, D. (2019). Bis (benzoxazol-2-yl) methanes Hounding NacNac: Varieties and Applications in Main Group Metal Coordination. *European Journal of Inorganic Chemistry*, *2019*(28), 3258–3264. https://doi.org/10.1002/ejic.201900631

Li, Y., Qian, F., Ge, X., Liu, T., Jalani, H. B., Lu, H., & Li, G. (2019). Copper and cobalt co-catalyzed aerobic oxidative cross-dehydrogenative coupling reaction of (benzo) azoles. *Green Chemistry*, *21*(21), 5797–5802. https://doi.org/10.1039/C9GC02464F

Liu, Q.-Q., Lu, K., Zhu, H.-M., Kong, S.-L., Yuan, J.-M., Zhang, G.-H., Chen, N.-Y., Gu, C.-X., Pan, C.-X., Mo, D.-L., & Su, G.-F. (2019). Identification of 3-(benzazol-2-yl)quinoxaline derivatives as potent anticancer compounds: Privileged structure-based design, synthesis, and bioactive evaluation in vitro and in vivo. *European Journal of Medicinal Chemistry*, *165*, 293–308. https://doi.org/10.1016/j.ejmech.2019.01.004

Mabkhot, Y. N., Barakat, A., Al-Majid, A. M., Alshahrani, S., Yousuf, S., & Choudhary, M. I. (2013). Synthesis, reactions and biological activity of some new bis-heterocyclic ring compounds containing sulphur atom. *Chemistry Central Journal*, *7*(1), 112 https://doi.org/10.1186/1752-153X-7-112

Madia, V. N., Messore, A., Pescatori, L., Saccoliti, F., Tudino, V., De Leo, A., Bortolami, M., Scipione, L., Costi, R., Rivara, S., Scalvini, L., Mor, M., Ferrara, F. F., Pavoni, E., Roscilli, G., Cassinelli, G., Milazzo, F. M., Battistuzzi, G., Di Santo, R., & Giannini, G. (2018). Novel benzazole derivatives endowed with potent antiheparanase activity. *Journal of Medicinal Chemistry*, *61*(15), 6918–6936. https://doi.org/10.1021/acs.jmedchem.8b00908

Matthews, C. J., Leese, T. A., Clegg, W., Elsegood, M. R., Horsburgh, L., & Lockhart, J. C. (1996). A route to bis (benzimidazole) ligands with built-in asymmetry: Potential models of protein binding sites having histidines of different basicity. *Inorganic Chemistry*, *35*(26), 7563–7571. https://doi.org/10.1021/ic960777m

Monguchi, D., Yamamura, A., Fujiwara, T., Somete, T., & Mori, A. (2010). Oxidative dimerization of azoles via copper (II)/silver (I)-catalyzed CH homocoupling. *Tetrahedron Letters*, *51*(5), 850–852. https://doi.org/10.1016/j.tetlet.2009.12.016

Mosdam, T. (1983). Rapid colorimetric assay for cellular growth and survival: Application to proliferation and cytotoxic assay. *Journal of Immunological Methods*, *65*, 55–63. https://doi.org/10.1016/0022-1759(83)90303-4

Nasr-Esfahani, M., Mohammadpoor-Baltork, I., Khosropour, A. R., Moghadam, M., Mirkhani, V., & Tangestaninejad, S. (2013). Synthesis and characterization of Cu (II) containing nanosilica triazine dendrimer: A recyclable nanocomposite material for the synthesis of benzimidazoles, benzothiazoles, bis-benzimidazoles and bis-benzothiazoles. *Journal of Molecular Catalysis A: Chemical*, *379*, 243–254. https://doi.org/10.1016/j.molcata.2013.08.009

Noel, S., Cadet, S., Gras, E., & Hureau, C. (2013). The benzazole scaffold: A SWAT to combat Alzheimer's disease. *Chemical Society Reviews*, *42*(19), 7747–7762. https://doi.org/10.1039/C3CS60086F

Peng, C. C., Zhang, M. J., Sun, X. X., Cai, X. J., Chen, Y., & Chen, W. H. (2016). Highly efficient anion transport mediated by 1,3-bis(benzimidazol-2-yl)benzene derivatives bearing electron-withdrawing substituents. *Organic & Biomolecular Chemistry*, *14*(35), 8232–8236. https://doi.org/10.1039/C6OB01461E

Racané, L., Pavelić, S. K., Ratkaj, I., Stepanić, V., Pavelić, K., Tralić-Kulenović, V., & Karminski-Zamola, G. (2012). Synthesis and antiproliferative evaluation of some new amidino-substituted bis-benzothiazolyl-pyridines and pyrazine. *European Journal of Medicinal Chemistry*, *55*, 108–116. https://doi.org/10.1016/j.ejmech.2012.07.005

Reddy, G. M., Garcia, J. R., Reddy, V. H., Andrade, A. M., Camilo, A., Jr. Ribeiro, R. A. P., & Lazaro, S. R. (2016). Synthesis, antimicrobial activity and advances in structure-activity relationships (SARs) of novel trisubstituted thiazole derivatives. *European Journal of Medicinal Chemistry*, *123*, 508–513. https://doi.org/10.1016/j.ejmech.2016.07.062

Sato, S., Kajiura, T., Noguchi, M., Takehana, K., Kobayashi, T., & Tsuji, T. (2001). AJI9561, a new cytotoxic benzoxazole derivative produced by Streptomyces sp. *The Journal of Antibiotics*, *54*(1), 102–104. https://doi.org/10.7164/antibiotics.54.102

Sepehri, S., Soleymani, S., Zabihollahi, R., Aghasadeghi, M. R., Sadat, M., Saghaie, L., & Fassihi, A. (2017). Synthesis, biological evaluation, and molecular docking studies of novel 4-[4-arylpyridin-1 (4H)-yl] benzoic acid derivatives as anti-HIV-1 agents. *Chemistry & Biodiversity*, *14*(12), e1700295. https://doi.org/10.1002/cbdv.201700295

Shaker, R. M. (1999). One-pot synthesis of novel 1, 1′-and 1, 4-bridged bis-thiazolidinone derivatives and their antimicrobial activity. *Phosphorus, Sulfur, and Silicon and the Related Elements*, *149*(1), 7–14. https://doi.org/10.1080/10426509908037017

Siegel, R. L., Miller, K. D., & Jemal, A. (2019). Cancer Society, 2019. *CA: A Cancer Journal for Clinicians*, *69*(1), 7–34. https://doi.org/10.3322/caac.21551

Singh, M. P., Joseph, T., Kumar, S., Bathini, Y., & Lown, J. W. (1992). Synthesis and sequence-specific DNA binding of a topoisomerase inhibitory analog of Hoechst 33258 designed for altered base and sequence recognition. *Chemical Research in Toxicology*, *5*(5), 597–607. https://doi.org/10.1021/tx00029a003

Sun, J., Yuan, B., Hou, X., Yan, C., Sun, X., Xie, Z., Shao, X., & Zhou, S. (2018). Broadband optical limiting of a novel twisted tetrathiafulvalene incorporated donor–acceptor material and its ormosil gel glasses. *Journal of Materials Chemistry C*, *6*(31), 8495–8501. https://doi.org/10.1039/C8TC02364F

Thurston, D. E., Bose, D. S., Thompson, A. S., Howard, P. W., Leoni, A., Croker, S. J., Jenkins, T. C., Neidle, S., Hartley, J. A., & Hurley, L. H. (1996). Synthesis of sequence-selective C8-linked pyrrolo[2,1-c][1,4]benzodiazepine DNA interstrand cross-linking agents. *The Journal of Organic Chemistry*, *61*(23), 8141–8147. https://doi.org/10.1021/jo951631s

Ueki, M., Ueno, K., Miyadoh, S., Abe, K., Shibata, K., Taniguchi, M., & Oi, S. (1993). UK-1, a novel cytotoxic metabolite from Streptomyces sp. 517-02. *The Journal of Antibiotics*, *46*(7), 1089–1094. https://doi.org/10.7164/antibiotics.46.1089

White, A. W., Curtin, N. J., Eastman, B. W., Golding, B. T., Hostomsky, Z., Kyle, S., Li, J., Maegley, K. A., Skalitzky, D. J., Webber, S. E., Yu, X.-H., & Griffin, R. J. (2004). Potentiation of cytotoxic drug activity in human tumour cell lines, by amine-substituted 2-arylbenzimidazole-4-carboxamide PARP-1 inhibitors. *Bioorganic & Medicinal*

Chemistry Letters, *14*(10), 2433–2437. https://doi.org/10.1016/j.bmcl.2004.03.017

Wu, Q., Chen, Y., Yan, D., Zhang, M., Lu, Y., Sun, W. Y., & Zhao, J. (2017). Unified synthesis of mono/bis-arylated phenols via RhIII-catalyzed dehydrogenative coupling. *Chemical Science*, *8*(1), 169–173. https://doi.org/10.1039/C6SC03169B